Screening of the Effect of Surface Energy of Microchannels on Microfluidic Emulsification

Wei Li,† Zhihong Nie,† Hong Zhang,† Chantal Paquet,† Minseok Seo,† Piotr Garstecki,*,‡ and Eugenia Kumacheva*,†

Department of Chemistry, University of Toronto, Toronto, Ontario M5S 3H6, Canada, Institute of Physical Chemistry, Polish Academy of Sciences, Kasprzaka 44/52, 01-224 Warsaw, Poland

Received February 28, 2007. In Final Form: April 18, 2007

We report the results of a systematic study of the effect of the surface energy of the walls of microchannels on emulsification in parallel flow-focusing microfluidic devices. We investigated the formation of water-in-oil (W/O) and oil-in-water (O/W) emulsions and found that the stability of microfluidic emulsification depends critically on the preferential wetting of the walls of the microfluidic device by the continuous phase. The condition for stable operation of the device is, however, different than that of complete wetting of the walls by the continuous phase at equilibrium. We found that W/O emulsions form when the advancing contact angle of water on the channel wall exceeds $\theta \approx 92°$. This result is unexpected because at equilibrium even for $\theta < 92°$ the microchannels would be completely wet by the organic phase. The criterion for the formation of W/O emulsions ($\theta > 92°$) is thus more stringent than the equilibrium conditions. Conversely, we observed the stable formation of O/W emulsions for $\theta < 92°$, that is, when the nonequilibrium transition to complete wetting by oil takes place. These results underlie the importance of pinning and the kinetic wetting effects in microfluidic emulsification. The results suggest that the use of parallel devices can facilitate fast screening of physicochemical conditions for emulsification.

Introduction

Microfluidic emulsification produces droplets[1] and bubbles[2] with a very narrow size distribution and controlled shapes and morphologies.[3] These droplets find applications in microreaction synthesis, in studies of protein crystallization, and in the continuous production of polymer and inorganic colloids.[4−6] Typically, water-in-oil (W/O) emulsions are produced in hydrophobic devices, and oil-in-water (O/W) emulsions are generated in hydrophilic droplet generators.[4a,7,8] An appropriate selection of the material of the microfluidic device is a critical step in microfluidic emulsification: if the droplet phase has a high affinity for the material of the microchannels, then it becomes a continuous phase leading to "phase inversion." A qualitative study suggests that for the stable formation of W/O emulsions the surface of the microchannels has to have a contact angle with water of 180°.[8]

Successful modifications of the surfaces of microchannels have been reported that allowed the formation of either W/O or O/W emulsions.[7] Furthermore, hydrophilic and hydrophobic devices connected in a series have been used for the generation of double emulsions.[9] Yet, in spite of the uttermost importance of the dependence of the formation of primary and double emulsions on the surface chemistry of the microchannels, there is no systematic study that addresses this issue.

In the present article, we examined the effect of surface energy on the emulsification of polar and nonpolar liquids. The study was carried out in a multichannel microfluidic droplet generator. The device contained four parallel flow-focusing devices (FFDs)[1c] with different surface energies. We report (i) the procedure for selective in-situ functionalization of the microchannels in parallel FFDs and (ii) the effect of surface modification of the channels on emulsification. We observed the stable formation of W/O and O/W emulsions or the failure of the microfluidic device to produce either kind of emulsion as a function of the surface energy of the microchannels.

* Corresponding authors. (E.K.) E-mail: ekumache@chem.utoronto.ca. (P.G.) E-mail: garst@ichf.edu.pl.

† University of Toronto.

‡ Polish Academy of Sciences.

(1) (a) Thorsen, T.; Reberts, R. W.; Arnold, F. H.; Quake, S. R. *Phys. Rev. Lett.* **2001**, *86*, 4163−4166. (b) Sugiura, S.; Nakajima, M.; Seki, M. *Langmuir* **2002**, *18*, 3854−3859. (c) Anna, S. L.; Bontoux, N.; Stone, H. A. *Appl. Phys. Lett.* **2003**, *82*, 364−366. (d) Nisisako, T.; Torii, T.; Higuchi, T. *Lab Chip* **2002**, *2*, 24−26. (e) Garstecki, P.; Fuerstman, M. J.; Stone, H. A.; Whitesides, G. M. *Lab Chip* **2006**, *6*, 437−446.

(2) (a) Loscertales, I. G.; Barrero, A.; Guerrero, I, Cortijo, R.; Marquez, M. Gañán-Calvo, A. M. *Science* **2002**, *295*, 1695−1698. (b) Garstecki, P.; Gitlin, I.; DiLuzio, W.; Whitesides, G. M.; Kumacheva, E.; Stone, H. A. *Appl. Phys. Lett.* **2004**, *85*, 2649−2651. (c) Marmottant, P.; Hilgenfeldt, S. *Proc. Natl. Acad. Sci. U.S.A.* **2004**, *101*, 9523−9527. (d) Guillot, P.; Colin, A. *Phys. Rev. E* **2005**, *72*, 066301−066304.

(3) (a) Nisisako, T.; Torii, T.; Takahashi, T.; Takizawa, Y. *Adv. Mater.* **2006**, *9*, 1152−1156. (b) Xu, S.; Nie, Z.; Seo, M.; Lewis, P. C.; Kumacheva, E.; Stone, H. A.; Garstecki, P.; Weibel, D. B.; Gitlin, I.; Whitesides, G. M. *Angew. Chem., Int. Ed.* **2005**, *44*, 724−728. (c) Nie, Z.; Li, W.; Seo, M.; Xu, S.; Kumacheva, E. *J. Am. Chem. Soc.* **2006**, *128*, 9408−9412. (d) Nie, Z.; Xu, S.; Seo, M.; Lewis, P. C.; Kumacheva, E. *J. Am. Chem. Soc.* **2005**, *127*, 8058−8063. (e) Zhang, H.; Tumarkin, E.; Peerani, R.; Nie, Z.; Sullan, R. M. A.; Walker, G. C.; Kumacheva, E. *J. Am. Chem. Soc.* **2006**, *128*, 12205−12210.

(4) (a) Cygan, J. Z. T.; Cabral, T.; Beers, K. L.; Amis, E. J. *Langmuir* **2005**, *21*, 3629−3634. (b) Hatakeyama, T.; Chen, D. L.; Ismagilov, R. F. *J. Am. Chem. Soc.* **2006**, *128*, 2518−2519. (c) Zheng, B.; Gerdts, C. J.; Ismagilov, R. F. *Curr. Opin. Struct. Biol*. **2003**, *13*, 538−544. (d) Poe, S. L.; Kobaslija, M.; McQuade, D. T. *J. Am. Chem. Soc.* **2006**, *128*, 15586−15587.

(5) (a) Chan, E. M.; Alivisatos, A.P.; Mathies, R. A. *J. Am. Chem. Soc.* **2005**, *127*, 13854−13861. (b) Nakamura, H.; Yamaguchi, Y.; Miyazaki, M.; Maeda, H.; Uehara, M.; Mulvaney, P. *Chem. Commu.* **2002**, *23*, 2844−2845. (c) Khan, S. A.; Gunther, A.; Schmidt, M. A.; Jensen, K. F. *Langmuir* **2004**, *20*, 8604−8611.

(6) (a) Nisisako, T.; Torii, T.; Higuchi, T. *Chem. Eng. J.* **2004**, *101*, 23−29. (b) Jeong, W. J.; Kim, J. Y.; Choo, J.; Lee, E. K.; Han, C. S.; Beebe, D. J.; Seong, G. H.; Lee, S. H. *Langmuir* **2005**, *21*, 3738−3741. (c) Dendukuri, D.; Tsoi, K.; Hatton, T. A.; Doyle, P. S. *Langmuir* **2005**, *21*, 2113−2116.

(7) (a) Okushima, S.; Nisisako, T.; Torii, T.; Higuchi, T. *Langmuir* **2004**, *20*, 9905−9908. (b) Barbier, V.; Tatoulian, M.; Li, H.; Arefi-Khonsari, F.; Ajdari, A.; Tabeling, P. *Langmuir* **2006**, *22*, 5230−5232.

(8) Dreyfus, R.; Tabeling, P.; Willaime, H. *Phys. Rev. Lett*. **2003**, *90*, 144505/1−144505/4.

(9) (a) Utada, A. S.; Lorenceau, E.; Link, D. R.; Kaplan, P. D.; Stone, H. A.; Weitz, D. A. *Science* **2005**, *308*, 537−541. (b) Nisisako, T.; Okushima, S.; Torii, T. *Soft Matter* **2005**, *1*, 23−27. (c) Okushima, S.; Nisisako, T.; Torii, T.; Higuchi, T. *Langmuir* **2004**, *20*, 9905−9908. (d) Barbier, V.; Tatoulian, M.; Li, H.; Arefi-Khonsari, F.; Ajdari, A.; Tabeling, P. *Langmuir* **2006**, *22*, 5230−5232.

10.1021/la7005875 CCC: $37.00 © 2007 American Chemical Society
Published on Web 06/21/2007

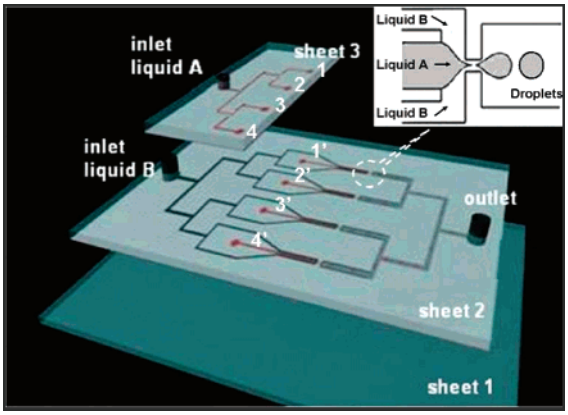

Figure 1. Illustration of the quadra droplet generator. The inset shows a schematic of the individual flow-focusing droplet generator.[1c] Sheet 1 is a nonpatterned sheet. Sheet 2 contains inlet B for the continuous phase (liquid B), which via a series of T junctions is split between the eight parallel microchannels. Sheet 1 contains inlet A for the liquid to be dispersed (liquid A), which is supplied to outlets 1−4 via several T junctions. When three sheets are sealed (following plasma etching of PDMS) so that outlets 1−4 and 1′−4′ are precisely superimposed, liquid A enters four parallel, identical flow-focusing droplet generators that are fabricated in sheet 2. In the present work, the width of the orifices and the height of the microchannels were 50 ± 2 and 150 ± 2 μm, respectively.

Experimental Section

Materials. All reagents used in the present work were purchased from Aldrich Chemical Co. (Canada) and were used without further purification.

Experimental Design. Figure 1 shows a 3D illustration of the microfluidic device comprising four parallel, identical flow-focusing droplet generators. The device was fabricated in poly(dimethyl siloxane) (PDMS) (Dow Corning) using a standard soft lithography method.[10] The microfluidic device was obtained by sealing three poly(dimethyl siloxane) (PDMS) sheets:[10] a planar nonpatterned bottom sheet 1, an intermediate sheet 2 with the relief features of four parallel FFDs, and the top "adapter" sheet 3. When three sheets were sealed, outlets 1−4 and 1′-4′ were superimposed, and liquid A entered four FFDs, all of which had the design shown in the inset of Figure 1. In each individual FFD, two immiscible liquids (deionized water and mineral oil mixed with 2 wt % Span 80 surfactant) were supplied to the central and side channels, respectively, or vice versa, as is shown in the inset of Figure 1. The liquids were introduced into inlets A and B using two separate syringe pumps (Harvard Apparatus). In the orifice, a thread of liquid A broke up and released droplets.[11] An optical microscope (Olympus BX41) coupled with a CCD camera (Evolution VF) was used to image the emulsification process. The distribution of the sizes of at least 200 droplets was determined by image analysis of the micrographs (Software Image-Pro Plus 5.0).

Surface Modification. The conditions of the surface modification of PDMS were first optimized by using planar polymer sheets. A PDMS sheet was immersed in a monomer solution (later referred to as monomer solution) with a particular composition and exposed to UV irradiation (Dr. Honle's UVA Print 40C, F-lamp, 400 W, λ = 330−380 nm), rinsed with deionized water, and dried.[12] Table 1 shows the compositions of the solutions used for the surface modification of PDMS.

Contact angles and the values of interfacial tension between the liquids were measured using a droplet shape analyzer (DSA100, Kruss). A sessile droplet with a volume of 3 μL was deposited on the surface of a PDMS sheet. Advancing and receding contact angles were measured with droplet volume increasing at a speed 5 μL/min. To measure surface and interfacial tensions, a pendant water or oil droplet was immersed in different media, such as air or water. Table 2 shows the values of advancing and receding contact angles of water and a mineral oil on the surface of PDMS in air.

(10) Xia, Y.; Whitesides, G. M. *Angew. Chem., Int. Ed.* **1998**, *37*, 550−575.
(11) Garstecki, P.; Stone, H. A.; Whitesides, G. M. *Phys. Rev. Lett.* **2005**, *94*, 164501/1−164501/4.
(12) Rohr, T.; Ogletree, D. F.; Svec, F.; Fréchet, J. M. J. *Adv. Funct. Mater.* **2003**, *13*, 264−270.

Table 1. Compositions of the Solutions Used for the Modification of PDMS Surfaces

monomer solution	benzophenone (g)	pluronic F-68 (g)	acrylic acid (g)	alcohol (g)	distilled water (g)	UV exposure time (min)
I	0.35	0.35	15	10[a]	75	5
II	0.30	0.30	15	30[b]	45	10
III	0.15	0.15	10	3.5[b]	35	5

[a] Isobutanol. [b] *tert*-Butanol.

Table 2. Contact Angle of Water and a 2 wt % Solution of SPAN 80 in Mineral Oil on the PDMS Surface

	FFD-1	FFD-2	FFD-3	FFD-4[a]
monomer solution (from Table 1)	I	II	III	
advancing contact angle of water,[b] θ_{WS}	80	92	105	112
receding contact angle of water[b]	65	73	93	99
contact angle of oil,[b] θ_{OS}	34	33	32	30
receding contact angle of oil[b]	16	18	19	18

[a] Nonfunctionalized PDMS surface. [b] All contact angles were measured in air.

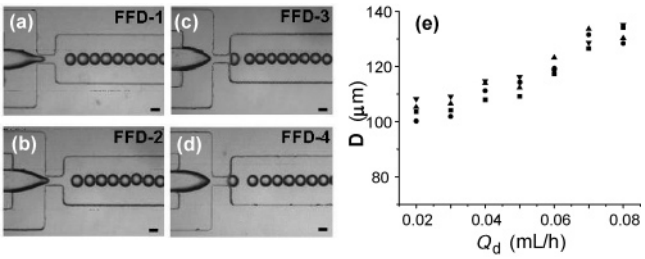

Figure 2. (a−d) Optical microscopy images of aqueous droplets generated in four parallel identical FFDs. In a−d, the flow rates of water and oil are 0.02 and 1.6 mL/h, respectively. The scale bar is 60 μm. (e) Variation of mean droplet size, *D*, plotted as a function of the flow rate of water. The flow rate of oil is 1.0 mL/h.

Results and Discussion

We first examined the emulsification of water (introduced as liquid A) in oil (introduced as liquid B) in four identical FFDs fabricated in nonmodified PDMS (Figure 2a−d). As expected from the hydrophobic nature of PDMS, emulsification produced a W/O emulsion. In the range of flow rates of water, Q_W, from 0.02 to 0.08 mL/h and flow rates, Q_d, of oil from 1.0 to 1.8 mL/h, the breakup of a thread of water occurred in a flow-focusing regime.[1c,11] The formation of droplets in four FFDs was reproducible: the size of the droplets generated in the individual FFDs did not differ by more than 3% (Figure 2e) (versus the difference of ca 2% for the droplets obtained in each FFD).

We then conducted selective graft polymerization of acrylic acid in the microchannels using the solutions and conditions specified in Tables 1 and 2. To modify one FFD at a time (e.g., FFD-1) the entire microfluidic device was filled with a particular monomer solution; however, only FFD-1 was exposed to UV irradiation. All other FFDs were protected from illumination with aluminum foil. After modification, the device was washed with deionized water. The procedure was repeated three times to functionalize FFD-1, FFD-2, and FFD-3. (FFD-4 was not modified.)

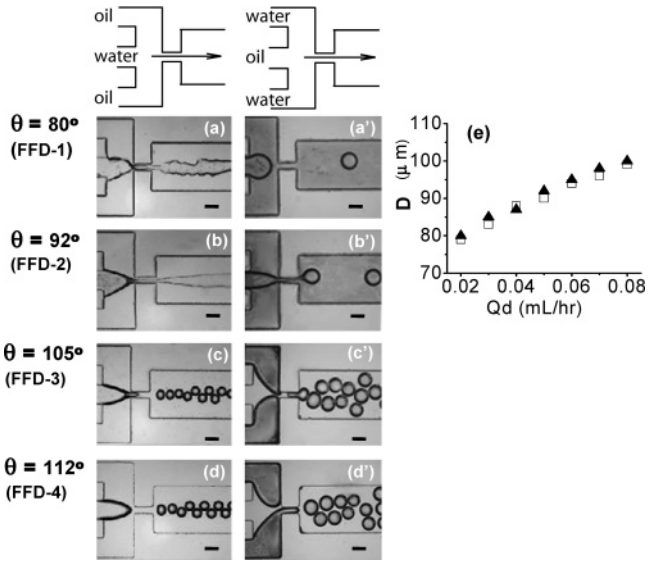

Figure 3. Optical microscopy images of microfluidic emulsification in four parallel FFDs with identical design but different surface energy: (a−d) liquids A and B are water and oil, respectively; (a′−d′) liquids A and B are oil and water, respectively. The water phase is labeled with a dye. The flow rates of water and oil are 0.02 and 1.6 mL/h, respectively. The scale bar is 100 μm. (e) Variation of diameter, *D*, of water droplets plotted as a function of the flow rate of water, as in c and d. (e) The flow rate of oil is 1.0 mL/h.

Functionalization of the surface of microchannels had several important consequences for the emulsification of water and oil. All effects described below were robust and reproducible, with no change for at least 6 to 7 h of emulsification.

Formation of W/O Emulsions. As follows from Figure 3a−d, when water was supplied as liquid A through the central channel, no emulsification occurred in the "hydrophilic" FFDs ($\theta = 80$ and 92°). The central stream of water extended into the downstream channel, wet the walls, and formed an interface with an erratic shape, suggestive of pinning (Figure 3a,b). In the "hydrophobic" FFDs with $\theta = 105$ and 112°, droplets were readily produced in the flow-focusing regime[1c] without partial wetting of PDMS by water (Figure 3c,d). The droplets were smaller than those obtained in the unmodified microchannels because the rate of flow of water through each of the four FFDs varied as a result of the different modes of operation.

The transition to emulsification occurred at $\theta > 92°$. This value of θ for the transition from partial wetting ($\theta < 92°$) to complete wetting ($\theta > 92°$) of the walls by the continuous phase was surprising: the calculation of the equilibrium contact angle of water surrounded by the organic phase suggested complete wetting of all of the substrates by oil, with water completely detached from the surface (Appendix A). We attribute the partial wetting of the channels with water for $\theta < 92°$ to the pinning of the liquid−substrate interface. Pinning is important when there is a considerable difference between the advancing and receding contact angles, characteristic of rough surfaces.[6,13,14] Pinning was also suggested by the erratic shape of the water stream that partially wet the surface of the functionalized PDMS (Figure 3a). More importantly, when oil completely wet the channel, the size of the water droplets did not depend on the surface energy of the microchannels, as shown in Figure 3c−e.

We note that the dynamics of breakup in each of the orifices in the multichannel device could be modified by coupling between the orifices, which could change the otherwise equal flow rates of liquids in the four FFDs. To examine a possible overlap between the feedback between the orifices and the effect of surface energy, a series of control experiments were carried out in which the emulsification of water was conducted in the *individual* (non-combined) FFDs that were modified as described above. In each device, the flow rates of water were from 0.005 to 0.02 mL/h, and the flow rates of oil were from 0.25 to 0.45 mL/h; that is, we used one-fourth of the flow rates of the oil and water phases supplied to the quadra droplet generator. Figure 4a−d shows representative images that were compared with images in Figure 3a−d, respectively. Qualitatively, the results were very similar to those obtained in the integrated multichannel device: in FFD-1 and FFD-2, the water thread wet the downstream microchannel, and in FFD-3 and FFD-4, aqueous droplets were produced with no significant difference in their dimensions. The diameters of droplets produced in the individual FFDs were typically 8−15 μm larger that those emulsified in the corresponding FFDs of the multiple droplet generator, suggesting that coupling indeed took place in the quadra droplet generator. This effect, however, did not contradict the observation made for the emulsification in the multichannel droplet generator, that is, the transition to the emulsification regime at $\theta > 92°$. This suggested that the parallel microfluidic device can be efficiently used for the fast screening of conditions for emulsification.

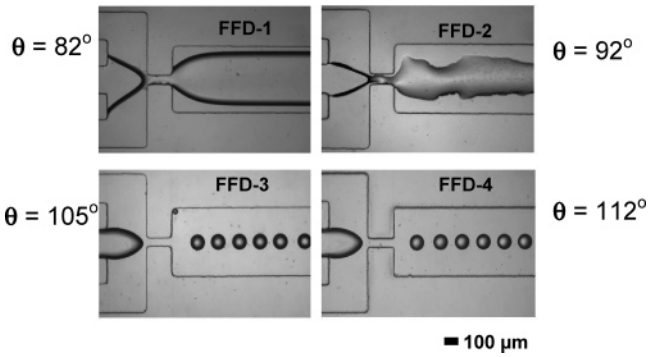

Figure 4. Optical microscopy images of emulsification in individual uncoupled FFDs. The flow rate of oil is 0.4 mL/h, and the flow rate of water is 0.005 mL/h.

Formation of O/W Emulsions. In the second series of experiments, oil was introduced into the central channel of the FFDs as liquid A, and water was supplied to the side channels of the FFDs as liquid B. No emulsification of oil occurred in the FFDs with $\theta = 105$ and 112° (Figure 3a′−d′). Instead, we observed "phase inversion": oil completely wet the walls of the FFD whereas water sheared off at the two corners of the side inlet channels and broke up into droplets, yielding W/O emulsions. For $\theta = 80$ and 92°, the stream of oil broke into droplets via a genuine flow-focusing mechanism (Figure 3a′,b′). The effects illustrated in Figure 3a′−d′ were observed in the range of flow rates of water from 0.02 to 0.08 mL/h and in the range of flow rates of oil from 1.0 to 1.8 mL/h. (We note that these ranges of flow rates were used to keep the formation of droplets in the flow-focusing regime and to avoid the formation of large droplets that acquired a nonspherical shape in the constrained geometry of microchannels.)

In summary, we conducted throughput screening of the effect of surface energy on microfluidic emulsification. The use of the prototype parallel flow-focusing device, together with the selective modification of the surface chemistry of the microchannels, proves to be an efficient method of screening the conditions for stable emulsification. Although coupling exists between the microchannels, our results show that the devices

(13) de Gennes, P. G. *Rev. Mod. Phys.* **1985**, *57*, 827−863.
(14) The rms roughness of unmodified and modified PDMS measured in air was 12 and up to 50 nm, respectively.

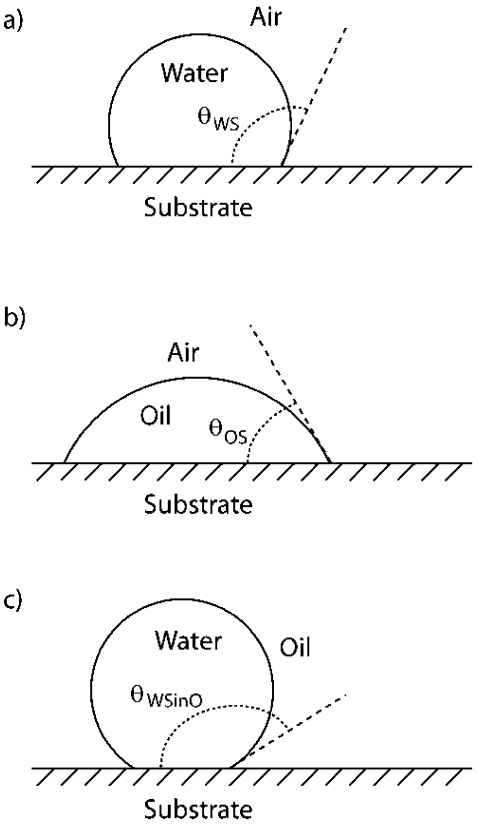

Figure 5. Droplets of (a, c) water and (b) oil on the PDMS substrate in (a, b) air and (c) oil.

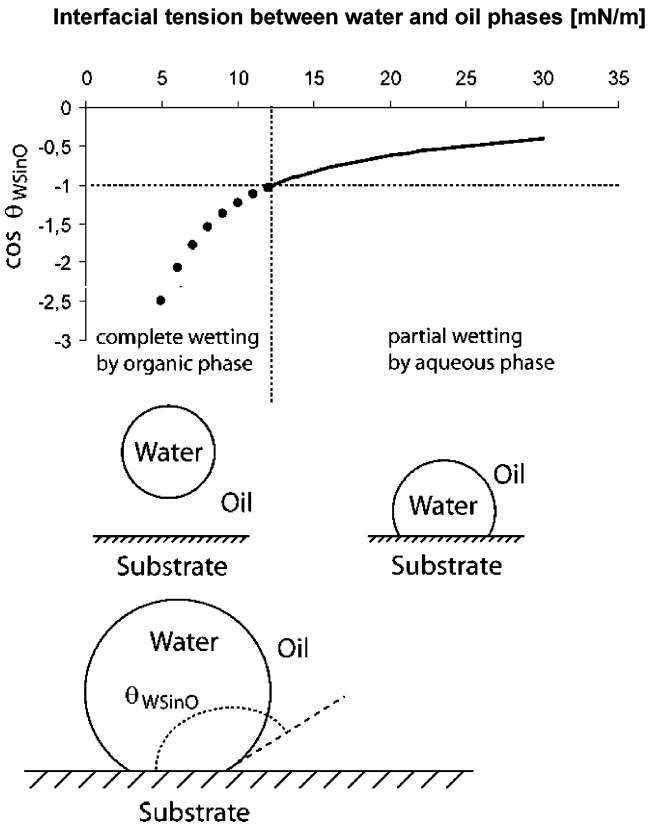

Figure 6. Variation of (the cosine of) the contact angle of water on the substrate in the surrounding organic phase plotted as a function of interfacial tension between water and oil.

can be used at least for the first fast assessment of the effect of wetting conditions on droplet emulsification.

We found that the emulsification of water occurs for $\theta > 92°$, following the transition to the nonwetting regime. This result was unexpected: under equilibrium conditions, the microchannels would be completely wet by the oil phase, with water completely detached from the surface. Thus, the nonequilibrium condition for the stable formation of W/O emulsions is more stringent than the equilibrium condition of complete wetting of the walls of the microfluidic device by the continuous organic fluid. Emulsification of oil occurs for $\theta < 92°$, when the nonequilibrium transition to complete wetting by oil takes place. This condition is less rigorous than the equilibrium one. These results underlie the importance of pinning and the kinetic effects in microfluidic emulsification. The criterion that we established here for the stable formation of W/O emulsions ($\theta > 92°$) is less stringent than $\theta \approx 180°$ reported earlier for smooth surfaces of the FFDs fabricated in glass.[11]

Appendix A

Calculation of the Equilibrium Contact Angle of Water on Four PDMS Substrates with Varying Surface Energies in the Continuous Organic Phase. Figure 5 shows a schematic representation of the water and oil droplets on the PDMS substrate in air and the surrounding oil phase (a 2 wt % solution of SPAN 80 in mineral oil), together with the notation for the measured (θ_{WS} and θ_{OS}) and calculated ($\theta_{WS\text{ in }O}$) contact angles.

For the contact angles formed by water and oil droplets in air, we write the Young−Dupré equation

$$\gamma_{WA}\cos(\theta_{WS}) = \gamma_{SA} - \gamma_{SW} \quad (1)$$

$$\gamma_{OA}\cos(\theta_{OS}) = \gamma_{SA} - \gamma_{SO} \quad (2)$$

where γ is the interfacial tension with the subscripts corresponding to the water (W), air (A), substrate (S), and oil (O) phases.

Subtraction of eq 2 from eq 1 yields

$$\gamma_{WA}\cos(\theta_{WS}) - \gamma_{OA}\cos(\theta_{OS}) = \gamma_{SO} - \gamma_{SW} \quad (3)$$

Assuming partial wetting of the substrate by water, we write Young's equation for the contact angle of water on the substrate in the surrounding organic phase (Figure 5c)

$$\gamma_{WO}\cos(\theta_{WS\text{ in }O}) = \gamma_{SO} - \gamma_{SW} \quad (4)$$

where $\theta_{WS\text{ in }O}$ is the contact angle of water on the substrate in the surrounding organic phase. Because the right-hand-side terms of eqs 3 and 4 are equal, after a simple transformation we can write

$$\cos(\theta_{WS\text{ in }O}) = \frac{\gamma_{WA}\cos(\theta_{WS}) - \gamma_{OA}\cos(\theta_{OS})}{\gamma_{WO}} \quad (5)$$

The measured values of interfacial tension are $\gamma_{OA} = 29$ mN/m and $\gamma_{WO} = 5$ mN/m. (For γ_{WA}, we used the standard value of 72 mN/m.[15]) The contact angles for the oil and water phases were taken from Table 2. By using $\theta_{OS} \approx 32°$ and by inserting the values of θ_{WS} from Table 1 into eq 5, we obtain $\cos(\theta_{WS\text{ in }O})$ values of −2.5, −5.4, −8.5, and −10.2 for $\theta_{WS} = 80$, 92, 105, and 112°, respectively. All values of $\cos(\theta_{WS\text{ in }O})$ are less than −1, indicating that the assumption of partial wetting of the substrate by water (eq 4) was incorrect.

(15) *Handbook of Applied Surface and Colloid Chemistry*; Holmberg, K., Ed.; John Wiley & Sons, 2002; Vol. 1.

As we explain below, this calculation leads to the conclusion that all four substrates that we tested experimentally are, at equilibrium, completely wet by the organic phase. This conclusion can be derived by plotting the variation of the value of cos($\theta_{WS\ in\ O}$) as a function of the value of the interfacial tension between the water and organic phases (keeping all other parameters constant). Figure 6 shows this variation for the least hydrophobic substrate ($\theta_{WS} = 80°$), along with schematics of water droplets under different conditions. At low values of γ_{WO}, complete wetting of the substrate with oil is observed (because the water−organic interface does not contribute very much to the surface energy), with water completely detached from the surface (case a). For higher values of γ_{WO}, partial wetting of the substrate by water is achieved (case b). On the basis of the calculations, for all substrates tested in the present work (with θ of 80, 92, 105, and 112°), the value of γ_{WO} at which the transition to wetting occurs is larger than the value measured experimentally ($\gamma_{WO} = 5$ mN/m). Thus, from the above calculation, we expect that, at equilibrium, all of the substrates that we tested experimentally are completely wetted by the organic phase.

Acknowledgment. We thank Materials Manufacturing Ontario and NSERC Canada for financial support of this work. P.G. thanks the Foundation for Polish Science for financial support.

LA7005875